Analytical Solution for Energy Management of Parallel Hybrid Electric Vehicles

Souad Hajd-Said, Guillaume Colin, Ahmed Ketfi-Cherif, Yann Chamaillard

Analytical Solution for Energy Management of Parallel Hybrid Electric Vehicles

S. Hadj-Said [*,**] **G. Colin** [**] **A. Ketfi-Cherif** [*] **Y. Chamaillard** [**]

[*] *Renault S.A.S, France (e-mail: souad.hadj-said@renault.com ; ahmed.ketfi-cherif@renault.com).*
[**] *Univ. Orléans, PRISME, EA 4229, F45072, Orléans, France (e-mail: guillaume.colin@univ-orleans.fr ; yann.chamaillard@univ-orleans.fr)*

Abstract: An analytical method is proposed to solve the optimization problem of energy management for a parallel hybrid electric vehicle. This method is based on Pontryagin's Maximum Principle (PMP) for a class of Hybrid Dynamic Systems (HDS). Therefore, the analytical models are used, which are an approximation of the reference models. A numerical method based on the reference models is also used in order to validate the analytical solution by comparing their results. In this paper, two types of optimization variables are considered: continuous and discrete. The first type is the power split between the Internal Combustion Engine (ICE) and the Electric Machine (EM). The second one is the transmission ratio, which includes the ICE On/Off decision. The results show that the analytical and the numerical solutions are almost the same. In addition, the analytical approach requires less computing time and requires less memory space than the numerical method.

Keywords: Energy Management Strategy, Hybrid Electric Vehicles (HEV), Analytical Method, Convex optimization, Pontryagin's Maximum Principle (PMP).

1. INTRODUCTION

In the automotive sector, the hybridization of the vehicle powertrain is considered as an alternative to reduce energy consumption and pollution emissions. Hybrid vehicles use at least two distinct types of power. Among them, the Hybrid Electric Vehicle (HEV) is composed of an internal combustion engine and one or more electric machines, as well as an energy buffer.

There are many approaches to design an optimal energy management strategy: deterministic Dynamic Programming (DP) (Pérez et al., 2006; Debert et al., 2010), stochastic DP (Johannesson et al., 2007), and Pontryagin's Maximum Principle (PMP) (Serrao et al., 2009; Kim et al., 2011; Stockar et al., 2011). While it is a globally optimal energy management, dynamic programming is computationally expensive, which limits its application to low-order systems (typically two states). The PMP offers the possibility to compact the optimization problem by defining the Hamiltonian function to handle the balance between the fuel cost and other related constraints, typically the battery state of charge. However, the main difficulty of the PMP method remains in finding the co-state.

The PMP method is widely used to solve in this area, analytically and numerically. In Elbert et al. (2014), the optimal torque split and the engine state On/Off were computed analytically using the PMP approach for a serial hybrid electric bus. Pham et al. (2016) proposed to calculate in addition the optimal EM On/Off analytically using the PMP, while in Nüesch et al. (2014), the engine On/Off and gearshift stategies were given numerically by a combination of DP and PMP. In this study, we focus on finding the optimal power split, engine state and gearshift analytically using PMP.

The objective of this paper is to find an energy management solution that minimizes the fuel consumed by the ICE. Therefore, an analytical solution, based on PMP, is proposed for energy management of a parallel HEV. The optimization variables are: the power split and the transmission ratio.

This paper is organized as follows. In section 2, the reference and the analytical models are presented. In section 3, the resolution of the optimization problem is proposed in two steps: first, the optimal power split and then the optimal transmission ratio. In section 4, the implementation of the analytical solutions is presented. In section 5, simulation results obtained analytically are compared to the results obtained numerically. The purpose of this comparison is to validate the analytical solutions.

2. VEHICLE MODEL

As shown in Fig. 1, the HEV configuration considered is a parallel HEV which consists of a battery, an electric motor, and an ICE delivering power to the wheels via a gearbox.

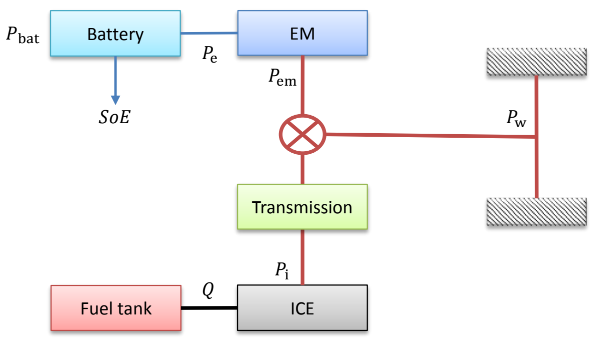

Fig. 1. Parallel HEV powertrain model

The wheel power P_w , demanded by the driver, is calculated from the vehicle speed set-point. So, the vehicle speed is considered as an input of the optimization, and is given by different cycles.

In the following the reference and approximated models of the different components are presented.

2.1 Reference Models

Engine The engine is modeled by the fuel flow (Q) consumed by the engine to deliver the mechanical power P_i.

$$Q(t) = \dot{m}_{fuel}(T_i(t), \omega_i(t)) \; [g/s] \tag{1}$$

where ω_i and T_i are the engine speed and torque. The mechanical power generated by the engine is expressed by: $P_i = T_i\omega_i \; [W]$ and limited by two functions of ω_i:

$$\underline{P_i}(\omega_i(t)) \leq P_i(t) \leq \overline{P_i}(\omega_i(t)) \tag{2}$$

Electric Motor (EM) The electric motor model expresses the electric power produced by the EM which includes the mechanical power delivered and the losses obtained from the specific power loss of the EM. So, the electric power P_e has the following expression:

$$P_e(t) = P_{em}(t) + loss(T_e(t), \omega_e(t)) \; [W] \tag{3}$$

with $P_{em}(t) = T_e(t)\omega_e(t) \; [W]$

The power P_{em} is limited by two functions of ω_e:

$$\underline{P}_e(\omega_e(t)) \leq P_{em}(t) \leq \overline{P}_e(\omega_e(t)) \tag{4}$$

Battery The battery is modeled as a resistive circuit (Badin, 2013; Murgovski et al., 2012) and the battery power is given by:

$$P_{bat}(t) = OCV(SoC)i_{bat}(t)[w] \tag{5}$$

$$P_{bat}(t) = P_e(t) + R_{bat}(SoC)i^2_{bat}(t) \tag{6}$$

The State of Charge (SoC) of the battery is defined as:

$$\dot{SoC}(t) = -\frac{i_{bat}(t)}{Q_{max}} \tag{7}$$

where $Q_{max}[C]$ is the maximal battery charge.

2.2 Analytical Models

Some assumptions and approximations were made to make the models analytical.

Engine The fuel flow Q is modeled by the "Willans Lines Model" as described in Rizzoni et al. (1999). Its analytical model is given by:

$$Q(P_i) = \begin{cases} a_1 P_i(t) + Q_0(t) & \text{if } \underline{P_i} \leq P_i \leq P_{lim} \\ a_2(P_i(t) - P_{lim}(t)) + Q_{lim}(t) & \text{if } P_{lim} \leq P_i \leq \overline{P_i} \end{cases} \tag{8}$$

where Q_0 is the idle fuel consumption.

where the parameters Q_0, P_{lim}, Q_{lim}, $\overline{P_i}$ and $\underline{P_i}$ are given as functions of ω_i:

$$Q_0(\omega_i(t)) = q_2\omega_i(t)^2 + q_1\omega_i(t) + q_0 \tag{9}$$

$$P_{lim}(\omega_i(t)) = p_1\omega_i(t) + p_0 \tag{10}$$

$$Q_{lim}(t) = a_1 P_{lim}(t) + Q_0(t) \tag{11}$$

$$\overline{P_i}(\omega_i(t)) = k_1\omega_i(t) + k_0 \tag{12}$$

$$\underline{P_i}(\omega_i(t)) = \frac{-Q_0(t)}{a_1} \tag{13}$$

and a_1, a_2 are assumed constant, where $a_1 >> a_2$.

Fig. 2 shows that the approximated engine model is sufficiently representative of the reference engine model.

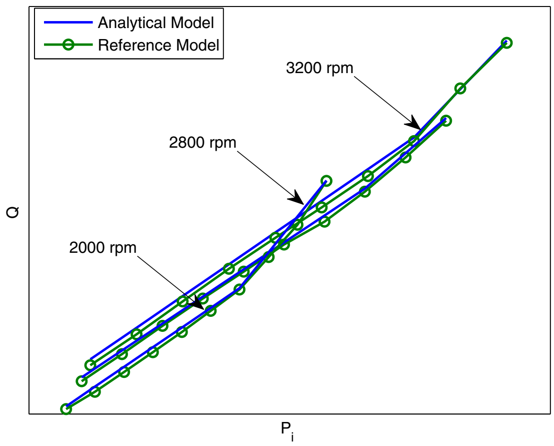

Fig. 2. Validation of the model of Q

EM and the Battery Concerning the electrical part, it is assumed that:

- The open circuit voltage (OCV) is constant
- The battery losses are neglected ($R_{bat}{i_{bat}}^2(t) \approx 0$)

Since the OCV is assumed constant, the State of Energy (SoE) can be used. It is given by:

$$\dot{SoE}(t) = -\frac{OCV i_{bat}(t)}{E_{max}} \tag{14}$$

where $E_{max} = OCVQ_{max}[J]$ is the maximal battery energy. The $SoE[\%]$ is limited by:

$$0 \leq SoE(t) \leq 100 \tag{15}$$

The analytical model of the battery power, which has been validated (Fig. 3), is given by:

$$P_{\text{bat}}(P_{\text{em}}) = \begin{cases} a_-(\omega_e)P_{\text{em}}(t) + b(\omega_e) & \text{if } \underline{P}_e \leq P_{\text{em}} \leq 0 \\ a_+(\omega_e)P_{\text{em}}(t) + b(\omega_e) & \text{if } 0 \leq P_{\text{em}} \leq \overline{P}_e \end{cases} \tag{16}$$

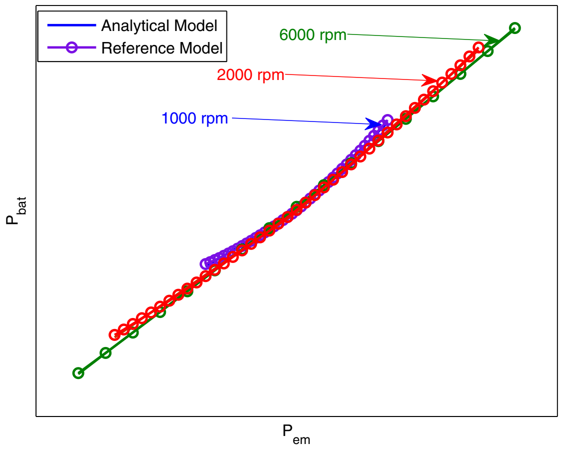

Fig. 3. Validation of the analytical model of P_{bat}

3. OFF-LINE OPTIMIZATION

In this section, the off-line optimization process is presented (Fig. 4). The outputs of this process are the optimal P_i (P_i^{opt}) and the optimal transmission ratio R_i (R_i^{opt}) which are calculated analytically. In this approach, P_i^{opt} is first calculated in steps 1 and 2, and R_i^{opt} is determined afterwards in step 3.

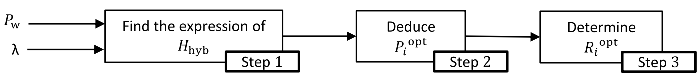

Fig. 4. Optimization Process

3.1 Continuous Control (Steps 1 and 2)

The optimization problem to determine P_i^{opt} is formulated as:

$$OP_A : \begin{cases} \min\limits_{P_i} \; J \\ \dot{SoE}(t) = -\dfrac{P_{\text{bat}}(t)}{E_{max}} \\ P_i + P_{\text{em}} = P_w \\ \underline{P_i} \leq P_i \leq \overline{P_i} \\ \underline{P}_e \leq P_{\text{em}} \leq \overline{P}_e \end{cases} \tag{17}$$

where

$$J = \int_{t_0}^{t_f} Q(P_i(t))dt \tag{18}$$

To find the optimal power split, the PMP is used. So, according to the PMP, minimizing J is equivalent to minimizing the Hamiltonian function which is calculated from (16) and (18), as follows:

$$H_{\text{hyb}}(P_i, P_w, \lambda) = Q(P_i) + \lambda(t)P_{\text{bat}}(P_{\text{em}}) \tag{19}$$

where λ is the Lagrange factor.

The Hamiltonian function H_{hyb} is the sum of two piecewise affine functions. So, to find P_i^{opt}, first, we have to calculate the expression of H_{hyb}. This is done by considering the points where the functions Q and P_{bat} change their slope. These points are $\underline{P_i}$, P_{lim}, P_w and $\overline{P_i}$.

The general expression of H_{hyb} is:

$$H_{\text{hyb}}(P_i) = A_1 P_i + A_0 + \lambda(B_1(P_w - P_i) + b)$$

The value of P_i which minimizes H_{hyb} is the optimum. So, the minimum of H_{hyb} depends on the sign of $(A_1 - \lambda B_1)$ which depends on λ and P_w. As shown in Fig. 5, if:

- $P_i < P_{\text{lim}}$ then $A_0 = Q_0$, $A_1 = a_1$
- $P_i > P_{\text{lim}}$ then $A_0 = Q_{\text{lim}} - a_2 P_{\text{lim}}$, $A_1 = a_2$
- $P_i < P_w$ then $B_1 = a_+$
- $P_i > P_w$ then $B_1 = a_-$

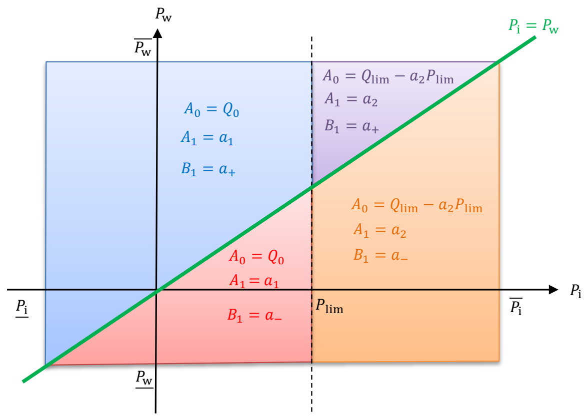

Fig. 5. Determination of the expression of H_{hyb}

Finally, as shown in Fig. 6, the three possible configurations of H_{hyb} are: increasing, decreasing or decreasing then increasing. Therefore, in each case, P_i^{opt} is deduced:

- $P_i^{\text{opt}} = \underline{P_i}$ for increasing form,
- $P_i^{\text{opt}} = \overline{P_i}$ for decreasing form,
- and $P_i^{\text{opt}} = P_{\text{lim}}$ or P_w for decreasing then increasing form.

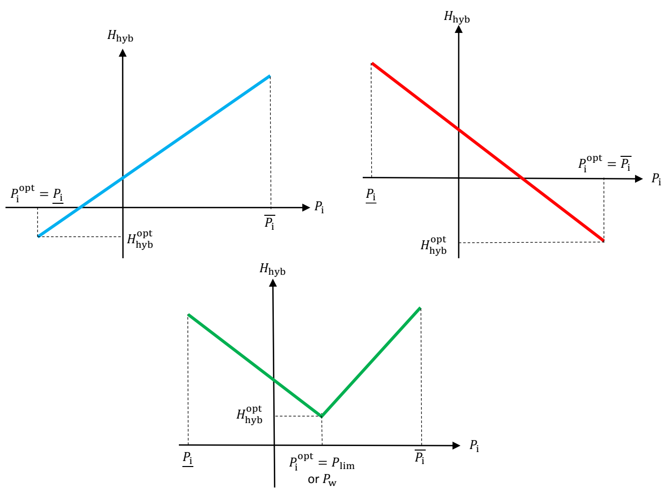

Fig. 6. Determination of P_i^{opt} according to the direction of variation of H_{hyb}

3.2 Discrete Control (Step 3)

The introduction of a discrete variable in the optimization problem P makes it hybrid from a mathematical point of view. For this kind of system, PMP can be applied (Riedinger, 1999). In Riedinger (1999), the author proposed a classification for hybrid dynamic systems (HDS) according to the nature of their hybridization and a modeling for each type. One of these types is HDS with controled hybridization. This kind of HDS corresponds to the studied system and its modeling, proposed by Riedinger (1999); Riedinger et al. (2003), is given in the following.

It is assumed that:

- $k \in K = \{1, 2, ..., N\}$ is the discrete control,
- $u_k \in U_k$ is the continuous control.

The system dynamics and the cost function are given by:

$$\dot{x} = f(x, u_k, k, t) = \sum_{k=1}^{N} m_k(t) f_k(x, u_k, t) \quad (20)$$

$$J = \int_{t_0}^{t_f} L(x, u_k, k, t) = \int_{t_0}^{t_f} m_k(t) L_k(x, u_k, t) \quad (21)$$

with $m_k = 1$ when k is the current mode; if it is not, $m_k = 0$.

By applying the PMP to the global system, the Hamiltonian function H is given by:

$$H(x, u_k, k, \lambda, t) = L(x, u_k, k, t) + \lambda f(x, u_k, k, t) \quad (22)$$

and in each mode k, the Hamiltonian function H_k is given by:

$$H_k(x, u_k, \lambda, t) = L_k(x, u_k, t) + \lambda f_k(x, u_k, t) \quad (23)$$

Finally, it was shown in Riedinger (1999) that the optimal control (k^*, u_k^*), which minimizes the function H, verifies:

$$H(x^*, u_k^*, k^*, \lambda^*, t) = \min_{k \in K}(\min_{u_k \in U} H_k(x, u_k, \lambda, t)) \quad (24)$$

The Optimal Transmission Ratio In step 3 of the process (Fig. 4), the PMP for HDS is applied in order to calculate the optimal transmission ratio. For example, if the set K is equal to $\{R_1, R_2\}$, with $\omega_i(R_1) < \omega_i(R_2)$, the corresponding Hamiltonian functions are:

$$H_{R_1}(x, u_{R_1}, \lambda, t) = L_{R_1}(x, u_{R_1}, t) + \lambda f_{R_1}(x, u_{R_1}, t) \quad (25)$$

$$H_{R_2}(x, u_{R_2}, \lambda, t) = L_{R_2}(x, u_{R_2}, t) + \lambda f_{R_2}(x, u_{R_2}, t) \quad (26)$$

The optimal transmission ratio is obtained by studying the sign of the difference
$H_{R_1}(x^*, u_{R_1}^*, \lambda^*, t) - H_{R_2}(x^*, u_{R_2}^*, \lambda^*, t) = \alpha(\lambda) P_w + \beta(\lambda)$

The expressions of α and β are determined in terms of λ.

Finally, as shown in Fig. 8, when:

- $P_w < P_{th}(\lambda)$, $H_{R_1} < H_{R_2}$ then $R_i^{opt} = R_1$,
- $P_w > P_{th}(\lambda)$, $H_{R_1} > H_{R_2}$ then $R_i^{opt} = R_2$,
- $P_w = P_{th}(\lambda)$, $H_{R_1} = H_{R_2}$. Where $P_{th}(\lambda) = \frac{-\alpha(\lambda)}{\beta(\lambda)}$ is the point of intersection of H_{R_1} with H_{R_2}.

This process could be done for a number of ratios greater than two.

4. ON-LINE OPTIMIZATION

This section describes how the analytical and numerical solutions are implemented. In both methods, λ^{opt} is assumed constant since the OCV dependence on SoE is neglected. λ^{opt} will be found by dichotomy.

4.1 Analytical Method

As shown in Fig. 7, P_i^{opt} is implemented in the form of a matrix, the lines are intervals of P_w and the columns are intervals of λ. Then, at an instant t, the expression of P_i^{opt} is found by placing $P_w(t)$ and $\lambda(t)$ with respect to these intervals.

Regarding R_i^{opt}, the formula of $P_{th}(\lambda)$ should be implemented. At an instant t, $P_w(t)$ is compared to $P_{th}(\lambda(t))$ to determine R_i^{opt} (Fig. 8). Here, four transmission ratios are considered: $R_i \in \{R_0, R_1, R_2, R_3\}$. The ratio R_0 corresponds to the engine Off, where, $L_0 = 0$ and $u_0 = 0$.

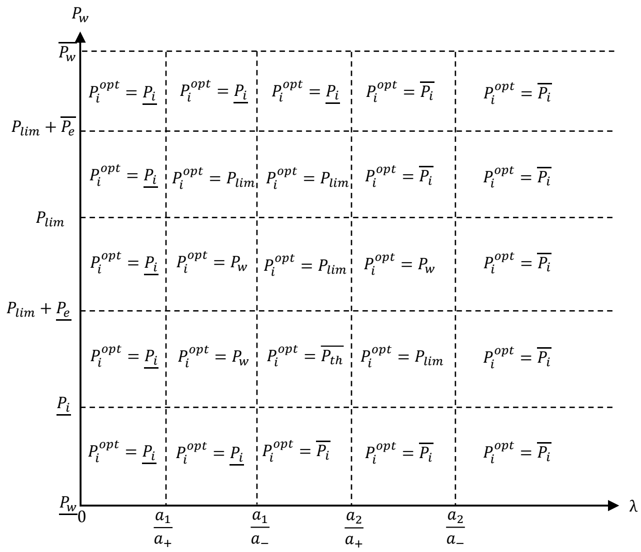

Fig. 7. Implementation of P_i^{opt} according to the values of P_w and λ

4.2 Numerical Method

The diagram in Fig. 9 explains the numerical approach to resolve OP_N (27) by applying PMP and using the reference models. First, at every instant t, the control P_i is meshed from the minimum $\underline{P_i}(t)$ to the maximum $\overline{P_i}(t)$. Then, the numerical value of $\overline{H}_{hyb}$ is calculated using the reference models of Q and P_{bat}. Finally, the optimal pair (P_i^{opt}, R_i^{opt}) is the one which corresponds to the minimum value of H_{hyb}.

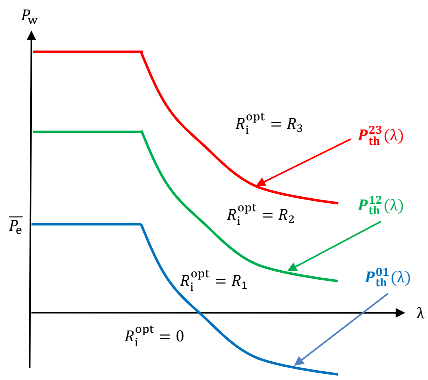

Fig. 8. Implementation of the limit $P_{th}(\lambda)$ which defines the optimal ratio

$$OP_N : \begin{cases} \min\limits_{P_i, R_i} H_{hyb}(P_i, R_i, P_w, \lambda) \\ S\dot{o}E(t) = -\dfrac{P_{bat}(t)}{E_{max}} \\ P_i + P_{em} = P_w \\ \underline{P_i} \le P_i \le \overline{P_i} \\ \underline{P_e} \le P_{em} \le \overline{P_e} \\ R_i \in \{0, R_1, R_2, R_3\} \end{cases} \quad (27)$$

where H_{hyb} is calculated from (1) and (6).

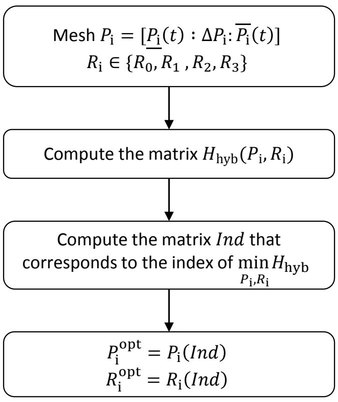

Fig. 9. Implementation of the numerical method

5. RESULTS

In this section, the fuel consumption and SoE trajectory results of the analytical method are compared to those of the numerical method in order to establish the performances of the analytical method. The fuel consumption value was obtained by applying the strategies on the reference model. Then, the robustness of the analytical solutions relative to the parameters Q_0 and P_{lim} is studied.

Table 1 shows that the analytical method has almost the same fuel consumption as the one found by the numerical method for all studied cycles. In addition, the averaged value of the computation time and memory space of the analytical method are lower than those of the numerical one.

Fig. 10 and 11 show that both methods provide a similar SoE trajectory and almost the same optimal control for the highway and urban cycles.

Cycle	**Strategy**	**FC [L/100km]**	**CPU [ms]**	**Memory [Bytes]**
ARTEMIS highway	Analytical	4.43	**1.55**	**88**
	Numerical	4.41	**17.38**	**704**
ARTEMIS urban	Analytical	3.29	**1.41**	**88**
	Numerical	3.25	**8.60**	**704**

Table 1. Fuel consumption, CPU time and Memory requirement results

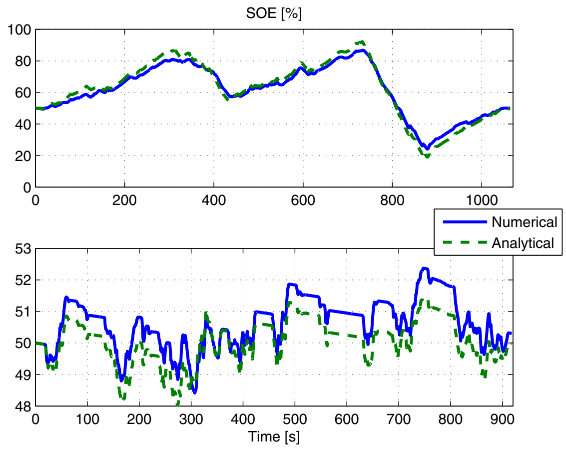

Fig. 10. Comparison of the SoE trajectory obtained by the numerical method and the analytical method for the highway cycle (top) and the urban cycle (bottom)

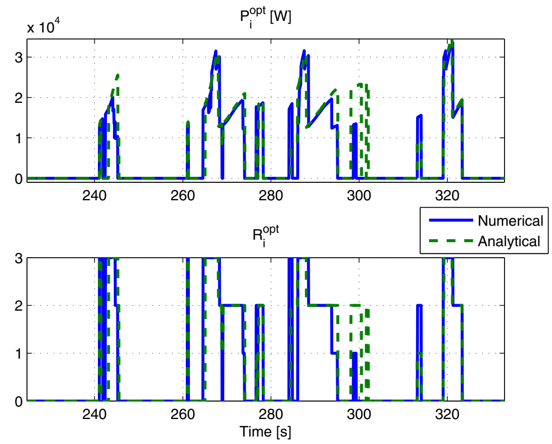

Fig. 11. A zoom of the optimal controls obtained by the numerical method and the analytical method for the ARTEMIS urban cycle

Robustness Analysis

Since the analytical model of Q is less accurate than that of the EM, the sensitivity evaluation of the analytical solutions (P_i^{opt}, R_i^{opt}) relative to the parameters Q_0 and P_{lim} is studied in the following.

The sensitivity, noted s, is measured by the difference in fuel consumption as follows:

$$s[\%] = 100 \times (\hat{Q} - Q) \quad (28)$$

where $\hat{Q}$, Q are respectively the fuel consumption corresponding to the control calculated with $(\hat{Q}_0, \hat{P}_{lim})$ and

$(Q_0, P_{\lim})$. It should be noted that the perturbation is inserted only in the strategy not in the model so that the comparison could be made.

The parameter perturbation is introduced by the factors α_{Q_0} and $\alpha_{P_{\lim}}$:

$\hat{Q}_0 = \alpha_{Q_0} \times Q_0$ and $\hat{P}_{\lim} = \alpha_{P_{\lim}} \times P_{\lim}$. If $\alpha < 1$, the parameter is underestimated, and if $\alpha > 1$, it is overestimated.

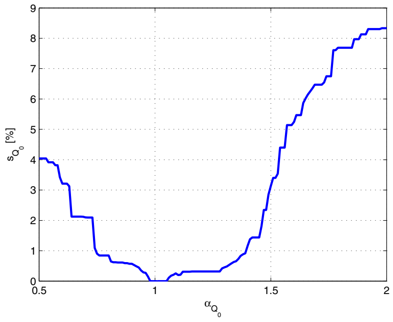

Fig. 12. Sensitivity of Q_0 for the ARTEMIS highway cycle

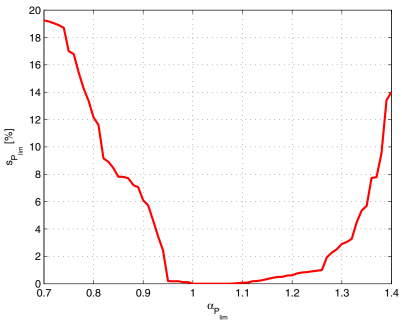

Fig. 13. Sensitivity of $P_{\lim}$ for the ARTEMIS highway cycle

Fig. 12 and Fig. 13 show that the sensitivity of the optimal control is very low for both Q_0 and $P_{\lim}$. In fact, an estimation error of $\pm 50\%$ in Q_0 causes an overcost less than 4%. Regarding $P_{\lim}$, an estimation error of $\pm 30\%$ causes an overcost less than 20%. This study aims to determine the tolerance interval of the model's parameters.

6. CONCLUSION

In this paper, an analytical approach has been presented and applied to calculate the energy management strategy for a parallel HEV. The results of the comparison show that the analytical method, which is based on analytical models, provides an optimal solution close to the one given by the numerical method, thereby validating the approximated models. The implementation of the analytical solutions is easier and requires less computing time than the numerical resolution. This encourages their use for embedded optimal control. Moreover, the results show that the analytical method is as efficient in the continuous case as in the discrete case. Finally, the results of the robustness analysis show that the analytical solutions are only slightly sensitive to the model parameter variations.

As perspectives, the analytical method will be applied to other HEV architectures (serial, serial/parallel), and to more complex configurations (several EM and batteries). This strategy will be implemented for real-time energy management. The robustness analysis can be extended to the parameters of the EM model.

REFERENCES

Badin, F. (2013). *Hybrid Vehicles*. Technip.

Debert, M., Colin, G., Chamaillard, Y., Mensler, M., Ketfi-cherif, A., and Guzzella, L. (2010). Energy management of a high efficiency hybrid electric automatic transmission. Technical report, SAE Technical Paper.

Elbert, P., Nuesch, T., Ritter, A., Murgovski, N., and Guzzella, L. (2014). Engine on/off control for the energy management of a serial hybrid electric bus via convex optimization. *Vehicular Technology, IEEE Transactions on*, 63(8), 3549–3559.

Johannesson, L., Asbogard, M., and Egardt, B. (2007). Assessing the potential of predictive control for hybrid vehicle powertrains using stochastic dynamic programming. *IEEE Transactions*.

Kim, N., Cha, S., and Peng, H. (2011). Optimal control of hybrid electric vehicles based on pontryagin's minimum principle. *Control Systems Technology, IEEE Transactions on*, 19(5), 1279–1287.

Murgovski, N., Johannesson, L., Sjöberg, J., and Egardt, B. (2012). Component sizing of a plug-in hybrid electric powertrain via convex optimization. *Mechatronics*, 22(1), 106–120.

Nüesch, T., Elbert, P., Flankl, M., Onder, C., and Guzzella, L. (2014). Convex optimization for the energy management of hybrid electric vehicles considering engine start and gearshift costs. *Energies*, 7(2), 834–856.

Pérez, L.V., Bossio, G.R., Moitre, D., and García, G.O. (2006). Optimization of power management in an hybrid electric vehicle using dynamic programming. *Mathematics and Computers in Simulation*, 73(1), 244–254.

Pham, T.H., Kessels, J.T.B.A., van den Bosch, P.P.J., and Huisman, R.G.M. (2016). Analytical solution to energy management guaranteeing battery life for hybrid trucks. *IEEE Transactions on Vehicular Technology*, 65(10), 7956–7971.

Riedinger, P. (1999). *Contribution à la commande optimale des systèmes dynamiques hybrides*. Ph.D. thesis.

Riedinger, P., Kratz, F., et al. (2003). An optimal control approach for hybrid systems. *European Journal of Control*, 9(5), 449–458.

Rizzoni, G., Guzzella, L., and Baumann, B.M. (1999). Unified modeling of hybrid electric vehicle drivetrains. *IEEE/ASME Transactions on Mechatronics*, 4(3), 246–257.

Serrao, L., Onori, S., and Rizzoni, G. (2009). Ecms as a realization of pontryagin's minimum principle for hev control. In *Proceedings of the American control conference*, 3964–3969.

Stockar, S., Marano, V., Canova, M., Rizzoni, G., and Guzzella, L. (2011). Energy-optimal control of plug-in hybrid electric vehicles for real-world driving cycles. *IEEE Transactions on Vehicular Technology*, 60(7), 2949–2962.